IET Microwaves, Antennas & Propagation

Research Article

IET Journals
The Institution of Engineering and Technology

Real-time high-resolution radio frequency channel sounder based on the sliding correlation principle

ISSN 1751-8725
Received on 24th March 2014
Accepted on 8th December 2014
doi: 10.1049/iet-map.2014.0165
www.ietdl.org

David Ferreira[1], *Rafael F.S. Caldeirinha*[1,2] ✉, *Nuno Leonor*[1]

[1]*Instituto de Telecomunicações (DL-IT), ESTG, Polytechnic Institute of Leiria, Leiria, Portugal*
[2]*Wireless and Optoelectronics Research and Innovation Centre, University of South Wales, Pontypridd, UK*
✉ *E-mail: rafael.caldeirinha@ipleiria.pt*

Abstract: A channel sounder based on the cross-correlation properties of pseudo-noise random sequences, known as swept time delayed cross-correlation channel sounder, is presented. This sounder enables the characterisation of doubly selective channels, providing both amplitude and Doppler spectra information. It performs real-time measurements of specific radio channels with a high resolution of 2 ns for adjacent multipath component, and a current maximum Doppler spread of ±100 Hz, but that can go beyond ±1 kHz, if some components are upgraded. The amplitude measurements given by the sounder, presented as power delay profiles, have a dynamic range of about 35–40 dB. This study provides detailed information on the most relevant components used to develop the sounder, and presents some of the calibration measurements performed on the bench, as well as specific radio frequency measurements at 18.7 and 60 GHz in a controlled environment. Finally, improvements that are feasible to be implemented in the near future are proposed.

1 Introduction

With the fast evolution of the information technologies, the need for larger system bandwidth becomes a pre-requisite for new and enhanced telecommunication systems and services. However, owing to the congestion radio spectrum witnessed at frequencies up to 3 GHz, higher frequency bands are, thus, required to accommodate the required bandwidth.

Indeed, the use of frequencies at micro- and/or millimetre wave frequencies is limited to radiowave propagation phenomena and channel impairments, which in turn are highly dependent on the deployed scenario and geometry. To this extent, appropriate studies aimed at the characterisation and modelling of the individual propagation mechanisms are critical for an effective planning and deployment of future wireless mobile and fixed communication systems.

In this paper, a real-time high-resolution radio frequency (RF) channel sounder, based on the swept time delayed cross-correlation (STDCC) technique, is presented. The proposed system topology allows for the characterisation of highly dynamic channels, enabling both amplitude and Doppler spectra measurements of the propagation channel. From the literature, similar channel sounders have already been implemented with different technical specifications and capabilities. For instance, in [1], the proposed sounder is limited to a time-delay resolution of 5 ns; whereas in [2], the system does not perform real-time correlation; in [3, 4], the sounders do not allow for Doppler spectrum measurements; and in [5], the sounder is reported with a 2.5 ns time-delay resolution, although it actually yields a 5 ns non-overlapping correlation pulse owing to the 400 MHz chip frequency used. And thus, a new topology based on high-speed digital-to-analogue converters (DAC) up to 1.25 GHz, in order to generate, download and transmit the desired pseudo-noise (PN) sequence, is proposed. In fact, the latter represents the main novelty of the proposed system as it allows one to have full control over the properties of the transmitted PN sequence, by uploading the desired vector into the DAC driver.

The integration of the proposed intermediate frequency stage into a highly scalable RF stage would represent an incremental step, particularly for a multi-frequency measurement system capable of measuring channel impulse response, in addition to the dynamic effects, including Doppler spectra for each individual multipath component (MPC), of doubly selective propagation channels. The proposed topology for the channel sounder has the portability to be quickly and easily re-locate to various measurement sites, as well as the flexibility to characterise a wide variety of frequencies that is 18 and 61 GHz. This is of significance interest for development of 5G propagation models.

The paper is organised as follows: Section 2 explains the principle behind the STDCC sounding technique; Sections 3 and 4 detail the transmitter and receiver blocks of the proposed sounder, respectively; Sections 5 and 6 depict the bench testing of the IF block and complete sounder, respectively; in Section 7 the Doppler capability of the sounder is assessed; in Section 8 a non-line-of-sight (NLOS) diffraction measurement setup in an anechoic chamber is presented; Section 9 depicts a multipath realistic measurement in anechoic chamber to assess the sounder multipath resolution; in Section 10 some conclusions are drawn; and finally, in Section 11, a few options for further improvement of the sounder are stated.

2 STDCC sounder theory

2.1 Sliding correlation principle

Channel sounding based on the sliding correlation technique was first demonstrated by Cox, in early 1970s [6]. This technique takes advantage of the auto-correlation properties of PN sequences, particularly those of the type of maximal length linear shift register [1, 2]. Such sequences, which can be generated using the underlying principle shown in Fig. 1*a*, have specific properties which are of great interest in the present application, namely [6, 7]: the statistical distribution of '1' and '0' is the same as in a purely random sequence, with the exception that the total number of '1' is greater in one unit to the total number of '0'; all the possible n-bit word combinations will appear in the sequence only once, with the exception of the n-zeros combination; the auto-correlation of a PN sequence is given by

$$R_{xx}(\tau) = -\frac{1}{N}\sum_{l=-\infty}^{l=+\infty}\left(1+\frac{1}{N}\right)\Delta\left(\frac{\tau - lNT_c}{T_c}\right) \quad (1)$$

© The Institution of Engineering and Technology 2015

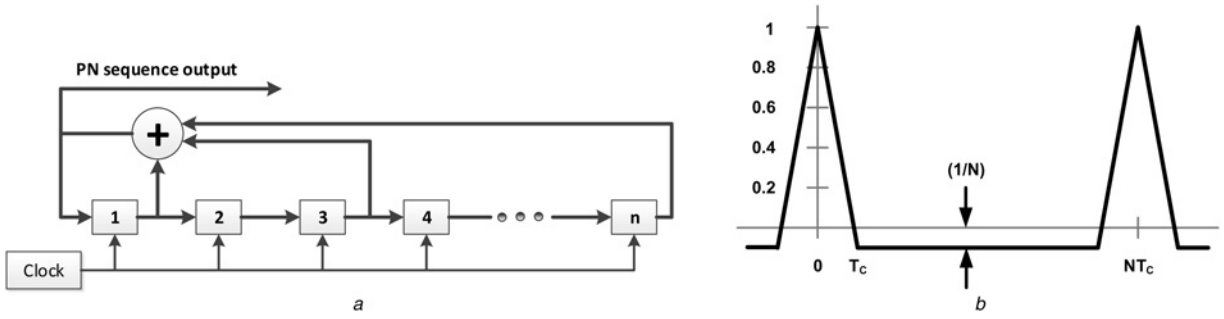

Fig. 1 *PN sequences*

a Example of a PN sequence generator
b Auto-correlation of a PN sequence

where

$$\Delta\left(\frac{\tau - lNT_c}{T_c}\right) = \begin{cases} 1 - \dfrac{|\tau - lNT_c|}{T_c}, & |\tau - lNT_c| \le T_c \\ 0, & |\tau - lNT_c| > T_c \end{cases}$$

T_c is the clock period, N is the PN sequence length, τ is the time delay and l defines the summation limits.

In order to have two sequences to 'slide' against each other, the receiver PN sequence clock needs to be adjusted to a slower rate than that of the PN clock at the transmitter. A maximum correlation amplitude will be obtained when both sequences are perfectly aligned in time, and a minima for all other cases [8]. Hence, distinct MPCs obtained from the radio channel will maximally correlate at different instants in time [1]. Fig. 1*b* depicts the auto-correlation of a PN sequence.

Despite the signal dispersion in time owing to multipath, in the order of several nanoseconds, the use of STDCC effectively spreads out in time those components at the output of the correlator [6]. The amount by which the correlation peaks are time dilated is described as sliding factor, denoted by

$$k = \frac{f_T}{f_T - f_R} \tag{2}$$

where f_T is the transmitter PN chip frequency and f_R is the receiver PN chip frequency. Consequently, when considering a transmitter PN sequence clocked at 100 MHz and a receiver PN sequence clocked at 99.999 MHz, which yields a sliding factor of 100 000, a 20 ns correlation pulse ($2T_c$) will be presented as a 2 ms pulse, representing the effective time dilation.

The theoretical dynamic range of a STDCC sounder, for a given power delay profile (PDP), can be specified as

$$D_R = 20\log_{10}(N_{PN})\ \text{(dB)} \tag{3}$$

where N_{PN} is the PN sequence length in chips [1].

2.2 Doppler spectra

In order to obtain Doppler spectra information of a radio channel, the receiver needs to acquire amplitude and phase information of the impulse response. In practice, this requires the implementation of a coherent receiver [1]. The output of the correlators can be combined to obtain the radio channel PDP and the phase response, according to (4) and (5), respectively

$$E(t) = |h(t,\tau)|^2 = f_I^2(t) + f_Q^2(t), \quad \text{time dilated by } k \tag{4}$$

$$\theta(t) = \angle h(t,\tau) = \tan^{-1}\left(\frac{f_Q(t)}{f_I(t)}\right), \quad \text{time dilated by } k \tag{5}$$

2.3 STDCC sounder parameters

The most relevant characteristics of a sounder implementing the sliding correlation technique are depicted in Table 1 [1, 8–10]. As one can see from Table 1, the chip period, as well as the PN sequence length, directly determines the main sounder characteristics. The sliding factor is also an important parameter, as it will determine the time scale dilation of the post-correlation signal, and therefore the type of equipment necessary to acquire that same signal. The dynamic range, the maximum detectable delay and the maximum Doppler shift denote some of the main sounder characteristics, and define the type of scenario where the sounder is to be used.

3 Sounder transmitter block

Fig. 2 presents the transmitter block diagram of the proposed sounder. The blocks of the IF stage were already described in [11, 12], and as such, only the remainder components will be detailed next.

3.1 10 MHz reference oscillator

The 10 MHz reference used throughout the measurements presented in this paper is from a E4407B spectrum analyser of Agilent. At the time of this paper this was the most stable reference present in the laboratory, although it is envisaged the acquisition of rubidium clock references in the near future, as is mentioned later in this paper.

3.2 RF PLL oscillator

The RF oscillator primarily used in the measurements, which was already available in the lab, is from Farran. This phase-locked dielectric resonator oscillator has an adjustable frequency that ranges from 18.2 to 18.8 GHz in 100 MHz steps. This component provides an output power of +13 dBm, and as an optional input

Table 1 STDCC sounder parameters and equations

Parameter	Symbol	Expression
chip period	T_c	$T_c = 1/f_c$ (s)
PN sequence length	N_{PN}	$N_{PN} = 2^n - 1$ (chips)
PN sequence period	T_{PN}	$T_{PN} = N_{PN}T_c$ (s)
RF bandwidth	B_{RF}	$B_{RF} = 2f_c$ (Hz)
base-band bandwidth (post-correlation)	B_{bb}	$B_{bb} = 2(f_T - f_R)$ (Hz)
sliding factor	k	$k = f_T/(f_T - f_R)$
theoretical dynamic range	D_R	$D_R = 20\log_{10}(N_{PN})$ (dB)
multipath time resolution	$\Delta\tau$	$\Delta\tau = 2T_c$ (s)
multipath spatial resolution	Δs	$\Delta s = c\Delta\tau$ (m)
maximum detectable delay	τ_{max}	$\tau_{max} = N_{PN}T_c$ (s)
maximum detectable distance	s_{max}	$s_{max} = c\tau_{max}$ (m)
maximum Doppler shift	f_{Dmax}	$f_{Dmax} = \pm(f_c/2kN_{PN})$ (Hz)
maximum detectable speed of an object	v_{max}	$v_{max} = \lambda_{carrier}/2kN_{PN}T_c$ (m/s)

IET Microw. Antennas Propag., 2015, Vol. 9, Iss. 8, pp. 837–846
© The Institution of Engineering and Technology 2015

17518733, 2015, 8, Downloaded from https://ietresearch.onlinelibrary.wiley.com/doi/10.1049/iet-map.2014.0165 by Instituto Politecnico De Leiria, Wiley Online Library on [18/10/2025]. See the Terms and Conditions (https://onlinelibrary.wiley.com/terms-and-conditions) on Wiley Online Library for rules of use; OA articles are governed by the applicable Creative Commons License

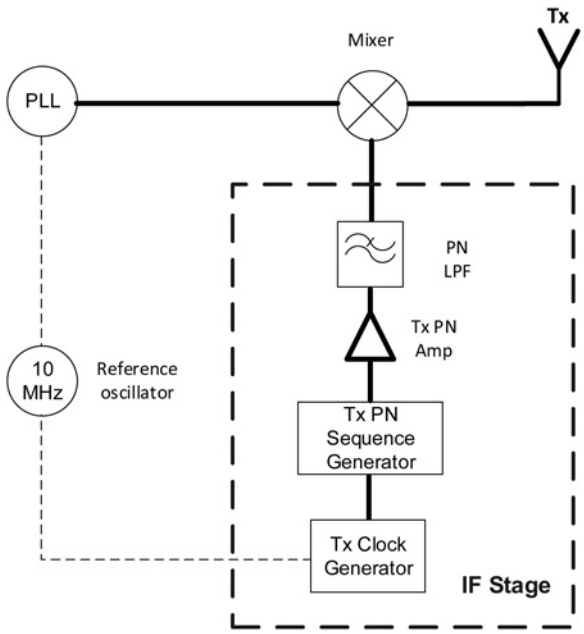

Fig. 2 *Sounder transmitter block*

connector for a 10 MHz reference. In IX, given the recent acquisition of 60 GHz hardware, 60 GHz measurements were also included.

3.3 Tx RF mixer

Owing to the constraints that arise from a diect downconversion to baseband, as it will be seen in the receiver block diagram, a single sideband mixer was used to mitigate such problem. A Miteq SM1819F09 W mixer with a RF local oscillator (LO) frequency range from 18.2 to 18.8 GHz and an IF range from 10 to 1000 MHz was used. The conversion loss for the allowed sideband is around 8 dB, and the rejected sideband yields to an attenuation around 30 dB.

4 Sounder receiver block

Fig. 3 depicts the receiver block diagram of the channel sounder. Similar to the transmitter block, the receiver IF stage blocks were also described in [11, 12]. The RF components are detailed next.

4.1 Rx RF mixer

To downconvert the RF signal to baseband, a double balanced mixer from Miteq was used. The DB0440HW1 presents an RF/LO range of 4–40 GHz and an IF range from DC to 2 GHz. The conversion loss for this mixer is between 6 and 8 dB.

4.2 Post-correlation

After correlation, the resulting signal needs to be amplified and filtered, in order to be properly detected by the data acquisition (DAQ). To this extent, specific electronic circuitry was developed, comprising two printed-circuit boards for the amplifier and filter components, respectively. A 12-pole switch was included so that pre-defined gains can be adjusted according to the specific dynamic range envisaged for a specific geometry/measurement. The gain of the post-correlation IQ signals can vary from 14 up to 19 dB, providing an appropriate level for the DAQ card input ports.

As per the low-pass filter, a seventh-order Chebyshev filter, with maximum theoretical ripple of 0.01 dB, and a cut-off frequency of

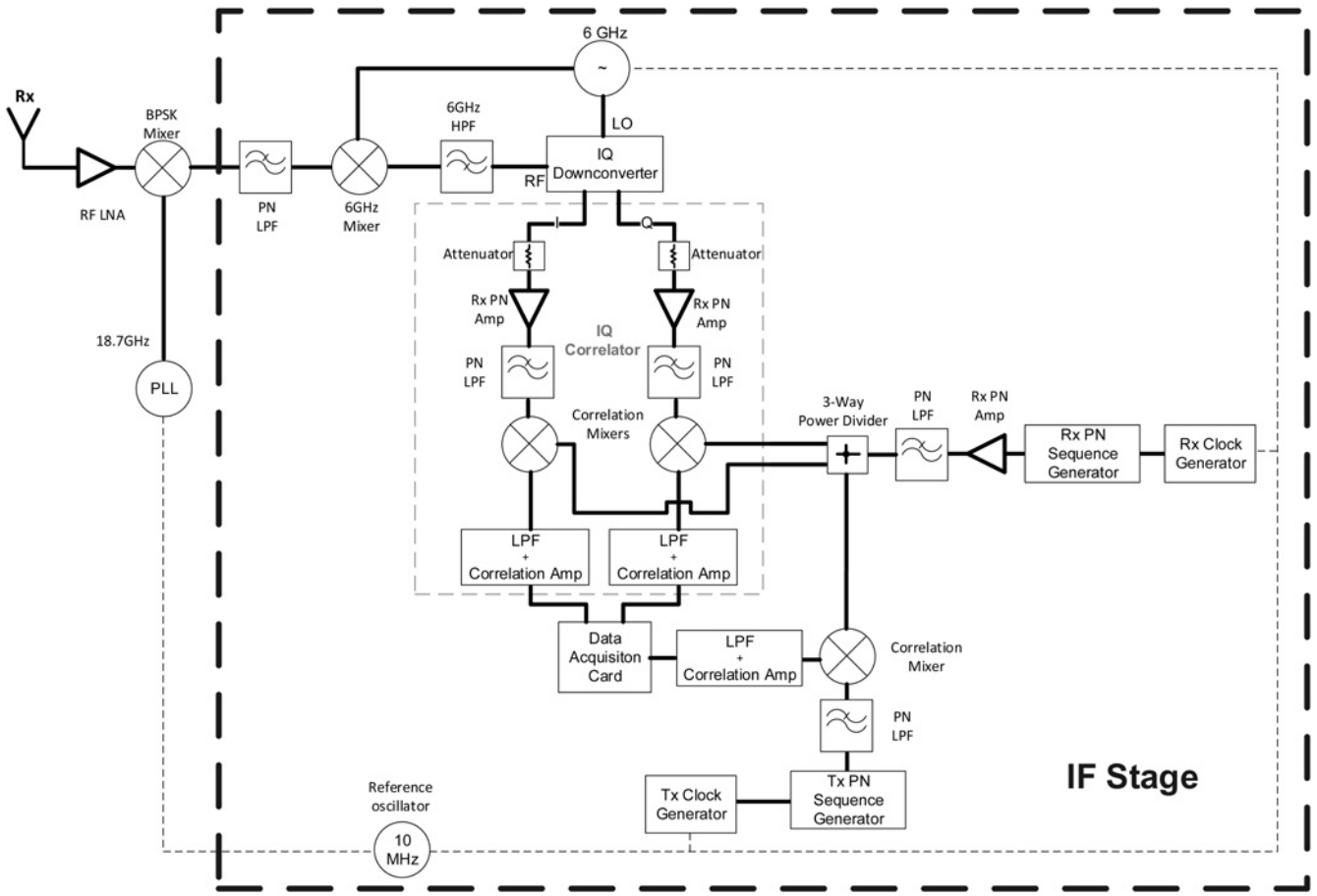

Fig. 3 *Sounder receiver block*

© The Institution of Engineering and Technology 2015

17518733, 2015, 8, Downloaded from https://ietresearch.onlinelibrary.wiley.com/doi/10.1049/iet-map.2014.0165 by Instituto Politecnico De Leiria, Wiley Online Library on [18/10/2025]. See the Terms and Conditions (https://onlinelibrary.wiley.com/terms-and-conditions) on Wiley Online Library for rules of use; OA articles are governed by the applicable Creative Commons License

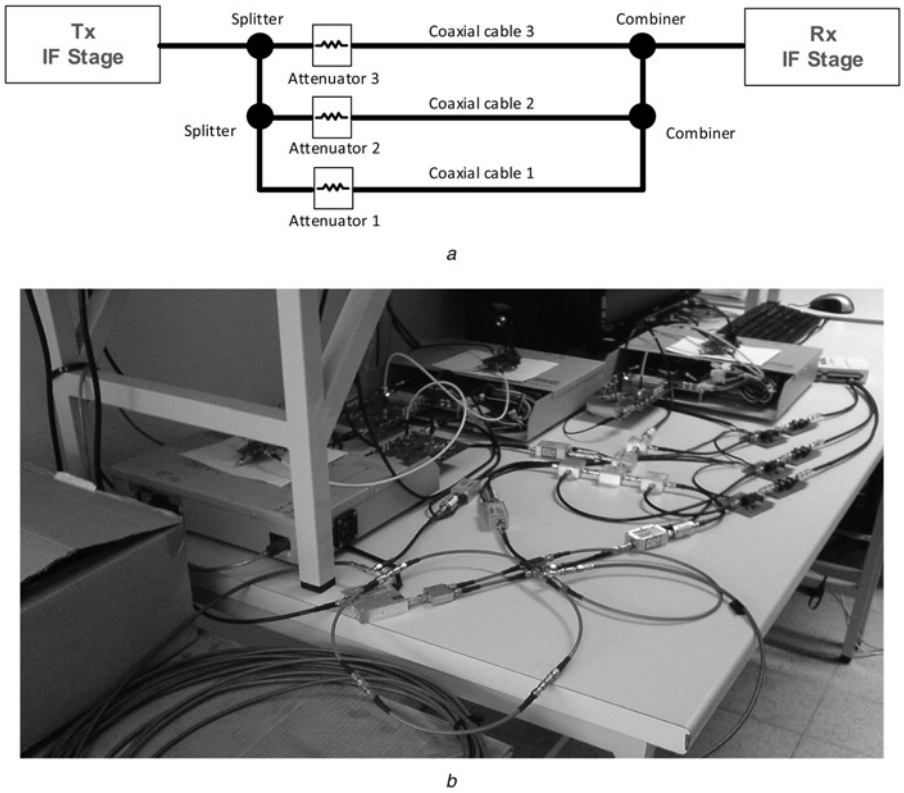

Fig. 4 *IF system*

a Depiction of the bench testing method
b Actual bench test

250 kHz, was implemented. This type of filter was chosen because of its steep roll-off, while minimising the pass-band ripple.

4.3 Data acquisition card

The acquisition of the correlation signals was done using an ordinary DAQ, that is NI USB-6211, from National Instruments, with 16 analogue inputs, a maximum symmetric input range of 10 V at a sampling frequency of 250 000 samples/s and 16 bits of resolution. Its sampling capability decreases proportionally with the number of signals to be acquired.

5 IF bench testing

5.1 Setup

Prior to full assembly of the sounder, several preliminary calibrations and measurements were carried out only on the IF system. These were performed for various coaxial cable lengths and attenuations, mimicking different multipath signal contributions, as shown in Fig. 4*a*. In Fig. 4*b*, both the testing environment and setup, which allowed one to properly evaluate the IF stage performance on multipath resolution and dynamic range, is depicted. Despite previous tests on the IF system, as detailed in [11, 12], emphasis will be given to two of them for convenience. Table 2 presents the main system specifications for this specific test. The results of the tests are presented in Table 3.

In the calibration process, cables/paths #1 and #3 were set to have the same physical length, so that path #2 will be used to assess the sounder multipath resolution, more specifically the resolution for consecutive multipath signals. Table 4 specifies the expected time delays for the signal travelling in paths #2 and #3 with respect to path #1.

Measurements were performed in order to assess the losses caused by the coaxial cables used, as well as the splitters/combiners, with the latter having approximately 3.4 dB of insertion loss.

Table 2 Main sounder specifications for bench test

Parameter	Value
transmitter PN chip frequency	1 GHz
receiver PN chip frequency	999.995 MHz
chip period	1 ns
PN sequence length	2047 chips
post-correlation signal bandwidth	10 kHz
maximum Doppler spread	1.22 Hz
sliding factor	200 000
theoretical dynamic range	66 dB
multipath time resolution	2 ns
multipath spatial resolution (cables)	0.42 m
maximum measurable delay	2.047 μs

Table 3 Paths simulated in each bench test

Test #	Cable 1, cm	Cable 2, cm	Cable 3, m	Att. 1, dB	Att. 2, dB	Att. 3, dB
1	20	60	15	20	30	15
2	20	50	15	20	30	15

Table 4 Expected time delays for multipath signals

Cable length	Time delay relative to path #1, ns
50 cm (path #2)	1.43
60 cm (path #2)	1.91
15 m (measured 14.89 m) (path #3)	69.95

© The Institution of Engineering and Technology 2015

17518733, 2015, 8, Downloaded from https://ietresearch.onlinelibrary.wiley.com/doi/10.1049/iet-map.2014.0165 by Instituto Politecnico De Leiria, Wiley Online Library on [18/10/2025]. See the Terms and Conditions (https://onlinelibrary.wiley.com/terms-and-conditions) on Wiley Online Library for rules of use; OA articles are governed by the applicable Creative Commons License

5.2 Measurement results

In this sub-section, results obtained for tests #1 and #2 are presented. Although measurements were obtained for both in-phase and quadrature signals, in the current analysis, for simplification, only one of these signals was assessed. Later in Section 6, on the full sounder measurements, both IQ signals were combined according to (4) and (5), followed by a new re-calibration of the system.

The system calibration, prior to executing the tests, will allow one to adjust the real-time data obtained by the DAQ card to an approximate power level for each MPC at the receiver input. For instances, the PN signal at the output of the transmitter PN generator, P_{Tx}, presented a power level of −5 dBm.

5.3 Test 1

This test aims at evaluating the theoretical time resolution of the sounder, that is 2 ns. The expected power levels for paths #1, #2 and #3 were observed to be −38.8, −49.2 and −33.8 dBm, respectively. The PDP is presented for test #1, in Fig. 5*a*. Fig. 5*b* presents results for only two first MPCs.

5.4 Test 2

In this specific test, the first two MPCs presented a time delay of 1.43 ns, which is, in a way, beyond the theoretical resolution of 2 ns. Similarly, the expected signal levels for paths #1 and #2 are −38.8 and −49.1 dBm, respectively. Results are depicted in Fig. 5*c*.

6 Complete sounder bench testing

The fully integrated sounder was tested in [13]. This was performed in a back-to-back bench method, as shown in Fig. 6*a*, with results depicted in Fig. 6*b*. In the latter, only a small time frame of the actual measurement is depicted. The two correlated path contributions actually correspond to the periodic repetition of the PN sequence being transmitted.

7 Doppler capability assessment

In order to assess the Doppler capability of the sounder, a controlled scenario was devised inside an anechoic chamber. To this extent, the transmitter box was placed at the one end of the anechoic chamber, whereas the receiver box was set to move in a straight line, at a constant speed, towards (away of) the transmitter. For a correct assessment of the retrieved Doppler information while considering the actual speed, the receiver was placed on top of a mobile robot, as shown in Fig. 7*a*. The receiver end was driven at a maximum linear speed of 510 mm/s.

The expected Doppler frequency can be obtained from (6), where θ_{Rx_Tx} is the internal angle between the receiver and transmitter vector, with the direction of travel vector

$$\text{Doppler}_{\text{freq}} = \frac{v_{\text{obj}}}{\lambda}\cos\left(\theta_{Rx\_Tx}\right) \tag{6}$$

For this test, the sounder parameters were changed so that the maximum Doppler spread was considerably higher than the expected values based on (6). Given this, Table 5 presents the sounder parameters used for this test.

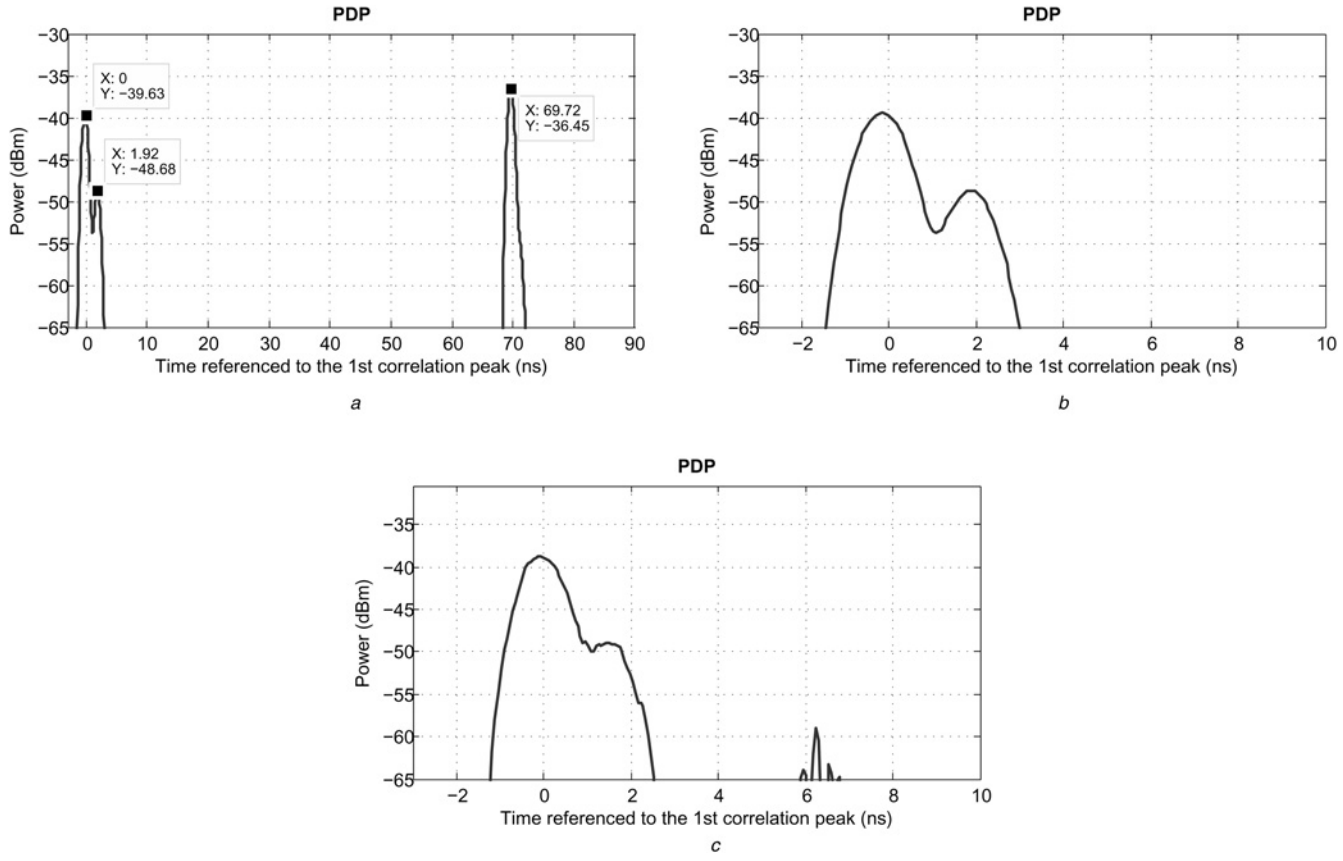

Fig. 5 *Measured PDP at receiver input port*

a Test 1
b Detail of test 1
c Test 2

© The Institution of Engineering and Technology 2015

17518733, 2015, 8, Downloaded from https://ietresearch.onlinelibrary.wiley.com/doi/10.1049/iet-map.2014.0165 by Instituto Politecnico De Leiria, Wiley Online Library on [18/10/2025]. See the Terms and Conditions (https://onlinelibrary.wiley.com/terms-and-conditions) on Wiley Online Library for rules of use; OA articles are governed by the applicable Creative Commons License

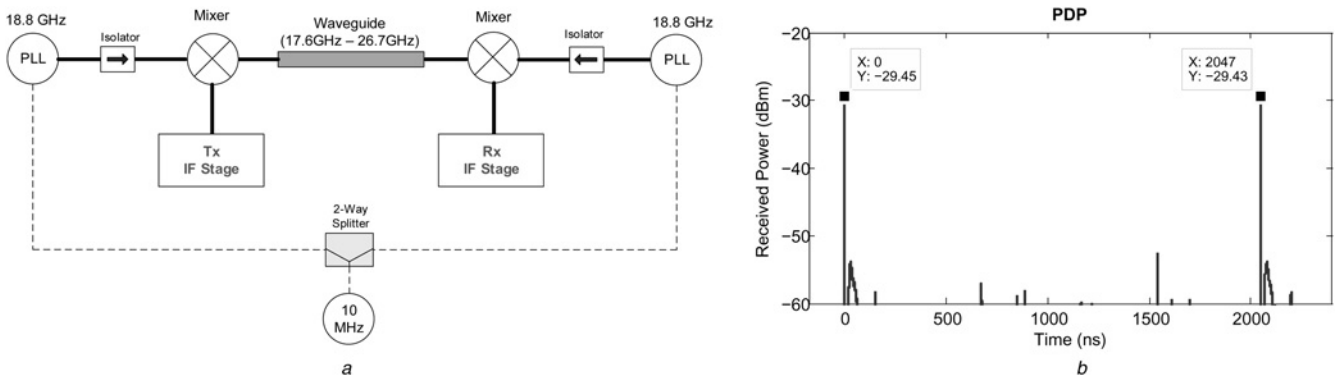

Fig. 6 *Testing of fully integrated sounder*

a Depiction of the test method for the fully integrated sounder
b Measured PDP for the RF bench test of the sounder

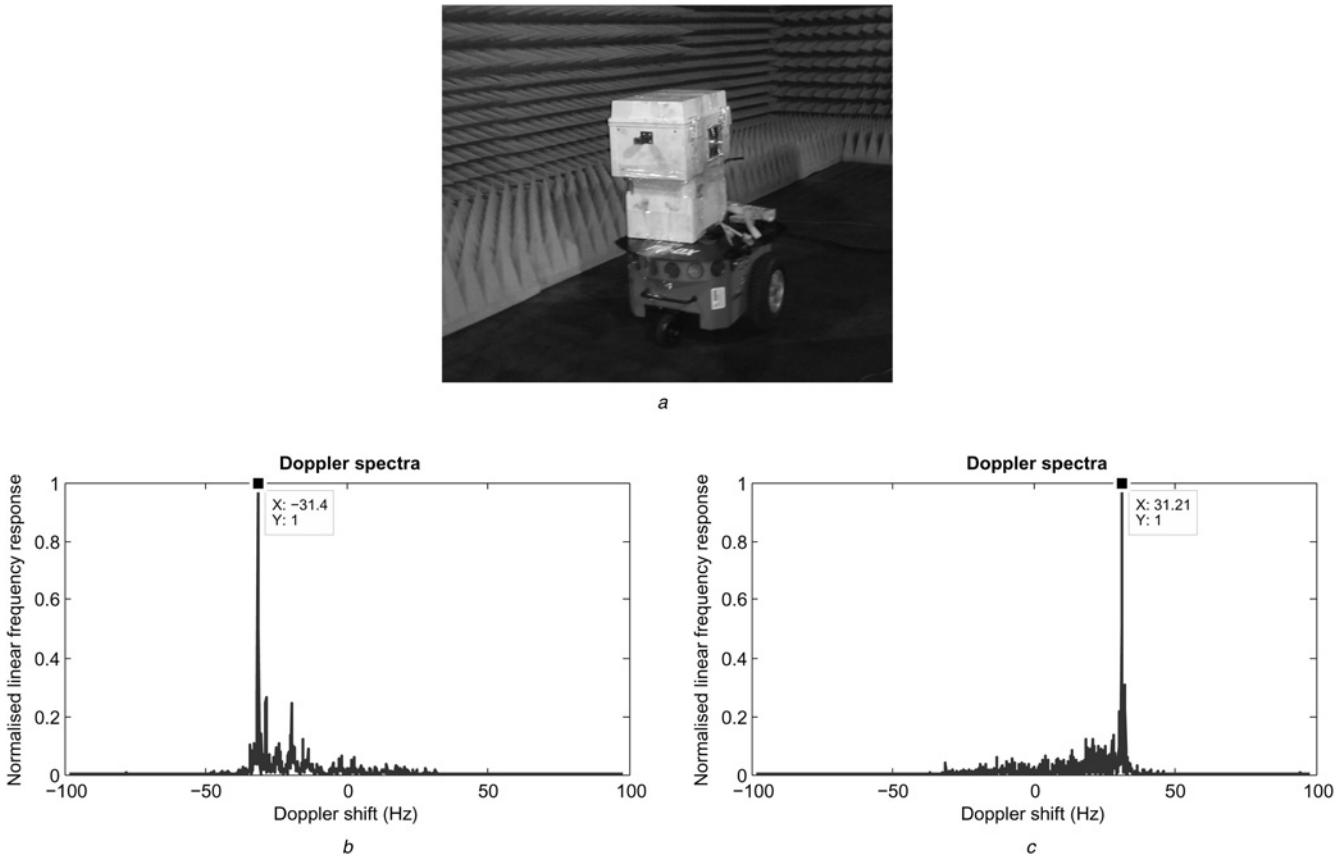

Fig. 7 *Doppler spectra measurements*

a Robot with receiver box on top
b Receiver moving away from the transmitter
c Receiver moving towards the transmitter

Table 5 Main sounder specifications for bench test

Parameter	Value
transmitter PN chip frequency	1 GHz
receiver PN chip frequency	999.950 MHz
chip period	1 ns
PN sequence length	255 chips
post-correlation signal bandwidth	100 kHz
maximum Doppler spread	98 Hz
sliding factor	20 000
theoretical dynamic range	48 dB

Several measurements were performed in a 3 m length straight path with direct line of sight, in which the receiver was set to move away from the transmitter and back. Fig. 7*b* shows the results of one of the measurements in which the receiver was moving away from the transmitter box. As it can be seen in this figure, there is a peak at −31.4 Hz, which differs from the expected theoretical value of −31.79 Hz. This can be explained by a slight depletion of the robots' batteries, which in turn makes it to move slightly below the set speed.

Similarly, Fig. 7*c* shows results for a measurement in which the receiver box was moving towards the transmitter box. As in

© The Institution of Engineering and Technology 2015

17518733, 2015, 8, Downloaded from https://ietresearch.onlinelibrary.wiley.com/doi/10.1049/iet-map.2014.0165 by Instituto Politecnico De Leiria, Wiley Online Library on [18/10/2025]. See the Terms and Conditions (https://onlinelibrary.wiley.com/terms-and-conditions) on Wiley Online Library for rules of use; OA articles are governed by the applicable Creative Commons License

Fig. 7*b*, the peak value of Fig. 7*c* is slightly lower than expected and also lower than the previous measurement, which again can be explained by the continuous depletion of the batteries.

Additionally, the sampling rate of the DAQ used is limited to 125 000 samples/s for two simultaneous channels. As such, and by adjusting the slip rate of the sequences as well as the PN sequence length, one can take the maximum Doppler spread to a little more than ±100 Hz, with a slight compromise in dynamic range. However, should a better DAQ unit be used instead, for example with a 1 MHz sampling rate, one could have a maximum Doppler spread of ±1 kHz for the same dynamic range, simply by changing the slip rate to 500 kHz.

8 NLOS diffraction assessment

With the purpose of assessing diffraction phenomena, a specific measurement campaign was devised in which the sounder was used to measure the receive signal envelope in a mobile scenarios, as depicted in Fig. 8. Two concrete slabs weighing 120 kg each (1 m × 1 m × 5 cm) were used. Slabs were positioned inside the anechoic chamber mimicking a building corner, as depicted in Fig. 8*b*. The transmitter was placed at 2 m from the building corner with an incident angle of 45°, and the receiver was moved by means of a rover from a NLOS to a line-of-sight (LOS) position, as depicted in Fig. 8*a*. In Fig. 8*c*, building corner diffraction measurement results were compared against results obtained from a ray tracing-based model proposed in [14]. From the analysis of the results, one may conclude that in the LOS region both measured and predicted results present a relatively good agreement. However in the NLOS zone, the model appears to underestimate the received signal as it was originally envisaged for reflection and diffraction propagation modes only. Despite the presence of a strong diffracted component in the NLOS case, results clearly indicate the presence of a double refracted component through the slabs, which in this case were physically relatively thin.

Although it was out of the scope of this paper to propose propagation models, a versatile radio channel sounder prototype with the capability of characterising the propagation channel through measurements of key channel indicators, for example Doppler spectra, channel impulse response at 18 and 61 GHz, will allow to build upon doubly selective channel models widely available in the literature. Consequently, refined and/or new models incorporating both channel time varying and multipath effects can be achieved. This would be accomplished through appropriate measurements of the radio channel for various geometries and frequencies. By considering the technical specifications of the proposed RF channel sounder, it will represent a significant improvement, both in volume and accuracy of the database presently available to system designers.

9 Multipath realistic measurement

For the correct assessment of the sounder ability to detect specific MPC, a measurement scenario was envisaged inside the anechoic chamber limited to the existing RF front-ends, at 18.7 and 60 GHz. This scenario consisted in placing several reflecting obstacles at defined locations, so that one could predict and confirm the arrival time for each of those MPC. Fig. 9*a* depicts two geometries used for this scenario, in which the difference relies only on the relative position of one of the obstacles with

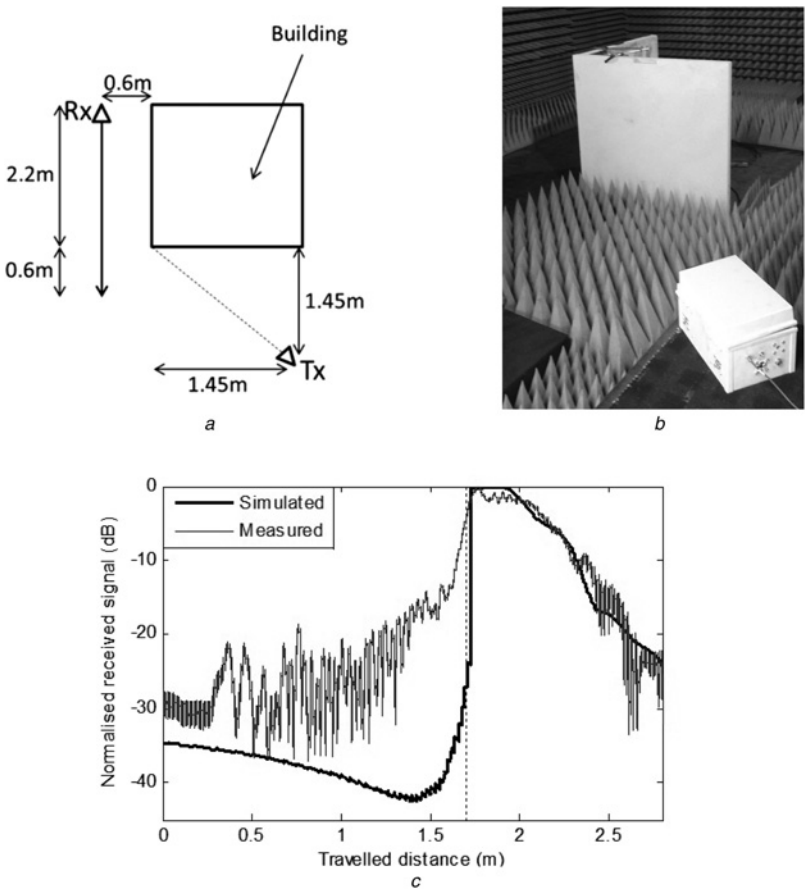

Fig. 8 *Corner diffraction NLOS measurement scenario*

a Measurement geometry
b Scenario setup in anechoic chamber
c Measurement results

© The Institution of Engineering and Technology 2015

17518733, 2015, 8, Downloaded from https://ietresearch.onlinelibrary.wiley.com/doi/10.1049/iet-map.2014.0165 by Instituto Politecnico De Leiria, Wiley Online Library on [18/10/2025]. See the Terms and Conditions (https://onlinelibrary.wiley.com/terms-and-conditions) on Wiley Online Library for rules of use; OA articles are governed by the applicable Creative Commons License

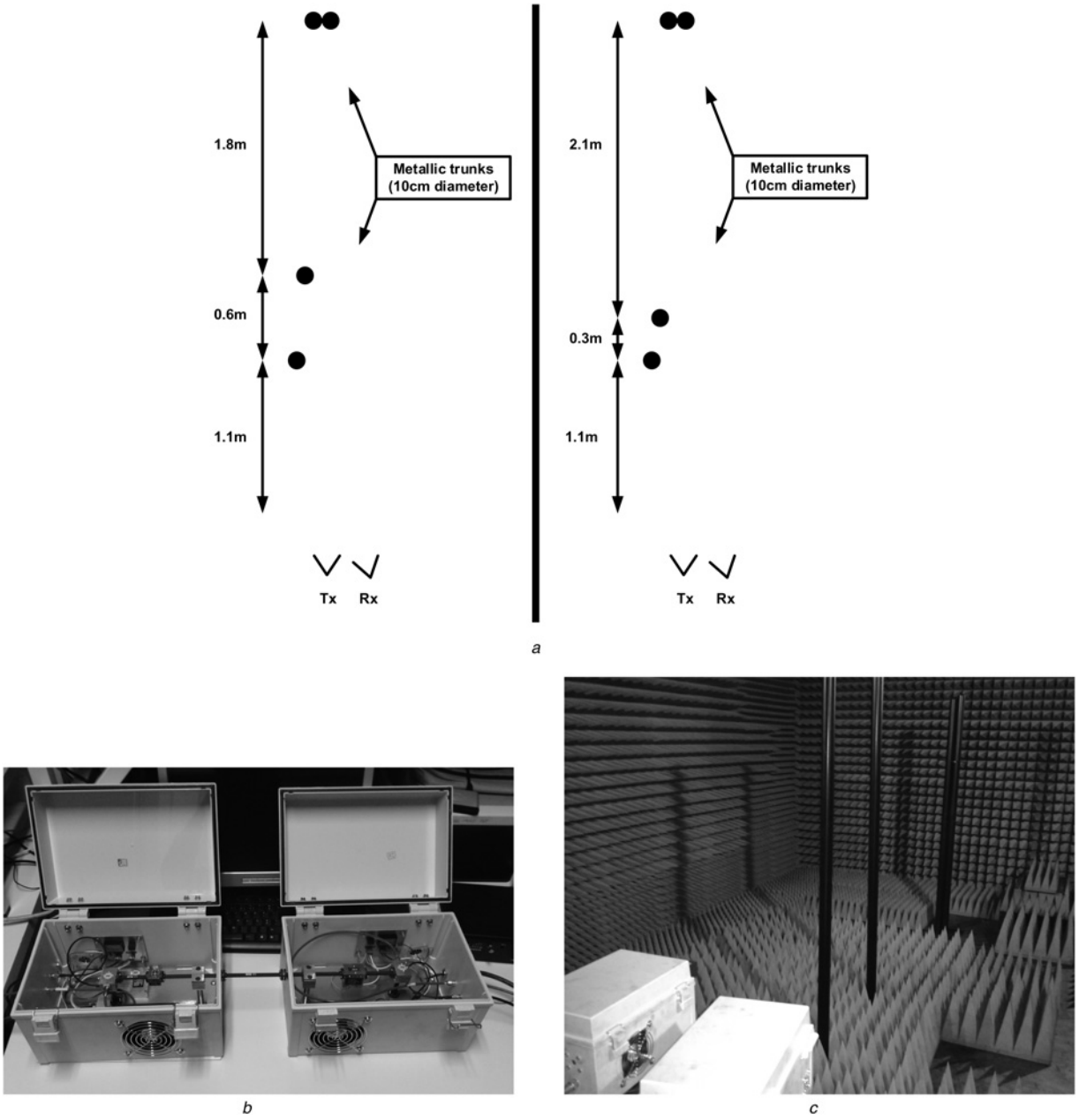

Fig. 9 *Measurement scenario for the correct assessment of the sounder performance*

a Measurement geometries inside anechoic chamber
b Back-to-back calibration of the 60 GHz front-end
c Measurement scenario for 60 cm variant

respect to the other. The obstacles used were metallic rods with 10 cm in diameter.

The sounder parameters used in these measurements are specified in Table 6. Since no moving obstacles were considered in the measurements, the slip rate and the chip length of the PN sequences were properly adjusted to yield an increased dynamic range of 66 dB.

From observing Fig. 9*a*, one can see that the multipath delay resolution of 2 ns will be assessed with the two closest trunks to the transmitter and receiver boxes. For the geometry variant where they are spaced out by only 30 cm, which corresponds to a total travel length difference of 60 cm, the MPC should retrieve 2 ns of travel time difference.

In Fig. 9*b*, one can see the back-to-back calibration procedure for the 60 GHz RF front-end, whereas in Fig. 9*c* the actual measurement setup inside the anechoic chamber for the 60 cm variant, is depicted.

9.1 18.7 GHz measurement results

Before presenting the actual PDP measurement results for the 18 GHz front-end, Table 7 presents the link budget of the system, excluding the channel path loss which is geometry dependent.

Table 6 Main sounder specifications for RF measurement

Parameter	Value
transmitter PN chip frequency	1 GHz
receiver PN chip frequency	999.975 MHz
chip period	1 ns
PN sequence length	2047 chips
post-correlation signal bandwidth	50 kHz
sliding factor	40 000
theoretical dynamic range	66 dB

© The Institution of Engineering and Technology 2015

17518733, 2015, 8, Downloaded from https://ietresearch.onlinelibrary.wiley.com/doi/10.1049/iet-map.2014.0165 by Instituto Politecnico De Leiria, Wiley Online Library on [18/10/2025]. See the Terms and Conditions (https://onlinelibrary.wiley.com/terms-and-conditions) on Wiley Online Library for rules of use; OA articles are governed by the applicable Creative Commons License

Table 7 Link budget for 18 GHz sounder

Parameter	Value
PN sequence power level	−5 dBm
PN to Tx mixer cable losses	5 dB
Tx mixer up-conversion losses	7.5 dB
Tx mixer to Tx antenna losses	2 dB
Tx antenna gain	20 dBi
Tx antenna −3 dB beamwidth	23°
Rx antenna gain	10 dBi
Rx antenna −3 dB beamwidth	63°
Rx RF LNA gain	38.5 dB
Rx RF LNA to mixer losses	1.7 dB
Rx mixer down-conversion losses	8 dB
Rx RF box to IF cable losses	4 dB

Table 8 Link budget for 60 GHz sounder

Parameter	Value
Tx mixer up-conversion losses	15 dB
Tx and Rx antennas gain	25 dBi
Tx and Rx antennas −3 dB beam width	10°
Rx RF LNA gain	28 dB
Rx mixer down-conversion losses	8 dB

After a few measurement runs to ensure proper alignment of both transmitter and receiver RF boxes, a PDP profile was extracted from each variant of the scenario, as shown in Figs. 10*a* and *b*, for the 60 and 30 cm variants, respectively.

From a close analysis of Fig. 10*a*, one can observe that all expected MPC are retrieved as follows: at 0 ns (closest trunk), 4 ns (middle trunk) and 16 ns (farthest set of trunks). However, an MPC can be detected from the same image at around 6 ns and another one resolved at 10 ns. Both of these MPC are due to double reflections between the first trunk and the RF boxes that consequently return towards the trunks and are viewed as secondary, lower power level, MPC.

From Fig. 10*b*, similar observations can be made about the discernible MPC, although the middle trunk is 30 cm closer to the RF boxes, and therefore is responsible for the MPC retrieved at 2 ns and around 8 ns. In this measurement, the 2 ns multipath delay resolution of the sounder can be further evaluated.

9.2 60 GHz measurement results

The link budget of the 60 GHz RF front-end is detailed in Table 8. To avoid information duplication, all the components that are shared with the 18 GHz RF front-end have been omitted from this table. The alignment of the RF boxes with the trunks proved to be more difficult than with the 18 GHz system, since narrower beamwidth antennas, that is 10° half power beamwidth, were used. With a good alignment in place, a number of PDP were extracted, being two of them visible in Figs. 10*c* and *d*, which correspond to the 60 and 30 cm variants, respectively.

In Fig. 10*c*, one can clearly see all three main MPC, and unlike the 18 GHz measurements, no double reflection MPC are visible. This is due both to the higher carrier frequency, which inherently means greater propagation losses and less reflected power levels, and also because of the narrower beamwidth of the antenna, meaning that the other MPC have a power level close or below the measurement set noise floor. By closely observing the visible MPC, one can see that the second MPC presents a higher power level than the first one. This is justified by the narrower antenna beamwidth, which meant that in order to clearly detect all the MPC, the RF boxes were pointed towards the middle trunk, hence

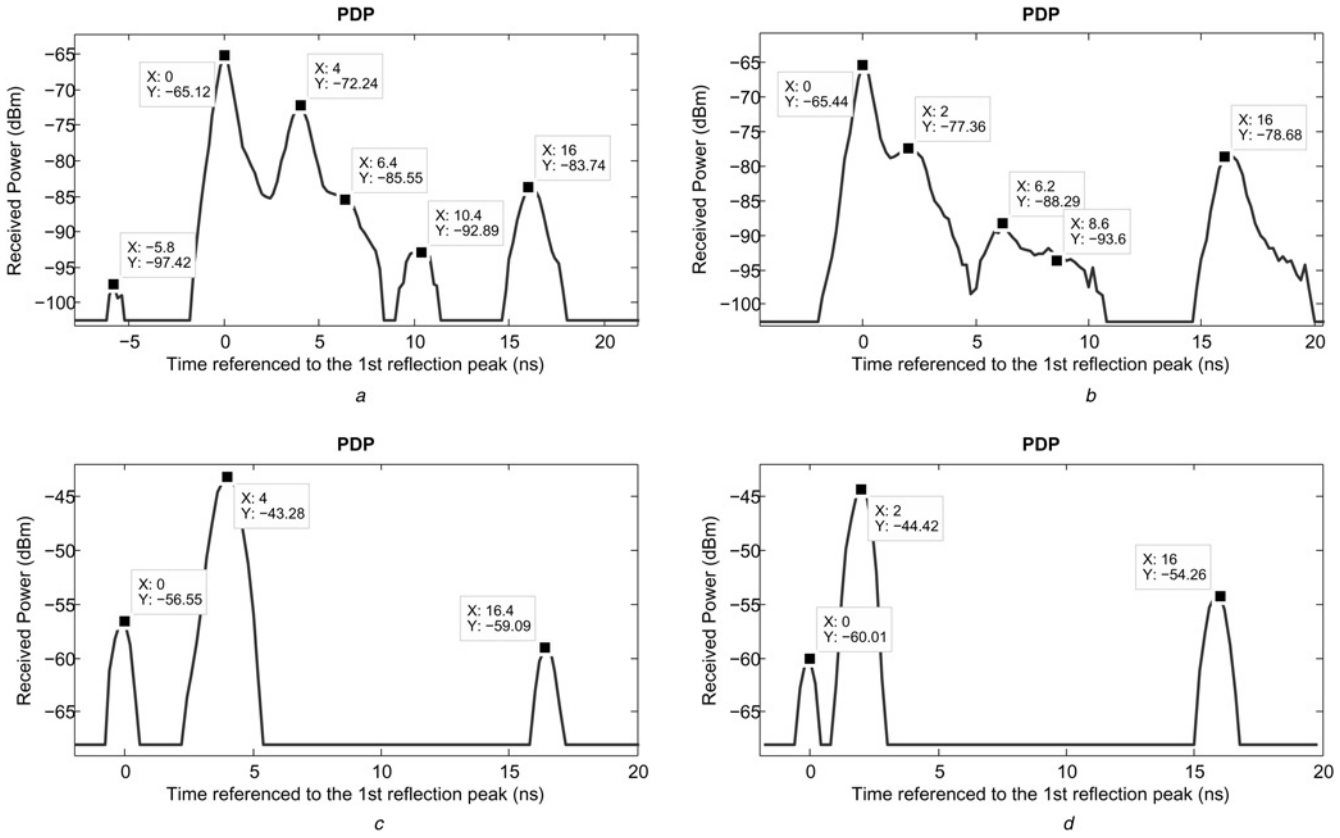

Fig. 10 *PDP profile for several measurements*

a 18 GHz, 60 cm variant
b 18 GHz, 30 cm variant
c 60 GHz, 60 cm variant
d 60 GHz, 30 cm variant

© The Institution of Engineering and Technology 2015

17518733, 2015, 8, Downloaded from https://ietresearch.onlinelibrary.wiley.com/doi/10.1049/iet-map.2014.0165 by Instituto Politecnico De Leiria, Wiley Online Library on [18/10/2025]. See the Terms and Conditions (https://onlinelibrary.wiley.com/terms-and-conditions) on Wiley Online Library for rules of use; OA articles are governed by the applicable Creative Commons License

giving it a higher power level, even when compared to the closest trunk.

Fig. 10*d* presents the results of the 30 cm spacing between the two closest trunks, and as expected, both of the corresponding MPC are clearly visible. Consequently, such results confirm the 2 ns consecutive multipath delay resolution as defined at the outset.

10 Conclusions

In this paper, an STDCC-based sounder by hardware and in real time was presented and assessed under several test conditions. From the results, one can conclude that the proposed sounder topology is able to successfully distinguish MPC spaced only by 2 ns. It has been shown that the Doppler shift values extracted from the dynamic measurements are in good agreement with the real object speed obtained from measurements. Although current maximum Doppler spread is limited to ±100 Hz, it can be easily extended to ±1 kHz by using a better data acquisition card. The overall unambiguous dynamic range under real measurement conditions, in which two closely spaced MPC can be successfully distinguished/resolved, was estimated to be around 35–40 dB for both 18 and 60 GHz RF front-ends.

The proposed sounder topology and implementation gathers all the different functionalities of previously reported STDCC sounders, while still outperforming them. The latter is derived from recent evolution in hardware performance. One of the main benefits of the proposed topology is in the use of the data pattern generator, allowing one to have full control over the PN sequence properties, so that the critical parameters that govern the performance of the sounder can be easily and quickly adjusted to the scenario/geometry under study.

Finally, a rather compact and highly portable channel sounder, as an alternative to a vector network analyser approach at IF stage [12], which is a major advantage to researchers that wish to study the channel across a variety of radio links. The mobility of such a system eliminates the need to disassemble, stow the equipment for transport and then re-assemble at the new site or measurement position. This is a lengthy process that requires time consuming and painstaking adjustments when setting up the equipment at the new location, and results in a significant amount of downtime during a measurements campaign.

11 Further work

Although the proposed topology provided good results for the conditions tested, further work can be performed to further improve the overall system performance, scalability and ease-of-use of the sounder.

On the one hand, the use of a better clock reference, that is rubidium, should provide better stability in the RF signal level under static conditions. Also, by having two of these clock references, coupled with the use of two GPS receivers capable of outputting 1 pulse per second (PPS), one can create a physical separation between transmitter and receiver sections. The 1 PPS of the GPS receivers would provide the required synchronisation for the rubidium references at both ends. On the other hand, the use of a better DAQ card would also improve the sounder in its Doppler measurement capability. This should allow for measurements under scenarios with fast moving objects/obstacles. Also, the integration with a sliding linear positioning system will allow one to fully automate measurement campaigns, particularly, in Synthetic Aperture Radar measurements. The current dynamic range of 40 dB can be further improved by appropriately choosing the transmitted PN sequence properties (which requires further studies) and by replacing some components, namely amplifiers and mixers in the IF subsystem, with ones with better specifications. Another option to increase the overall radio channel path loss of the sounder might be in the inclusion of a automatically/manually switched amplification section on the IF subsystem, in which amplifiers with different gains are appropriately selected depending on the specificities of the radio channel, therefore maximising the sounder performance.

12 Acknowledgments

This work was partially supported by Fundação para a Ciência e a Tecnologia (FCT), Portugal, under pluriannual funding and research project PTDC/EEATEL/099973/2008–ADCOD.

13 References

1 Anderson, C.R.: 'Design and implementation of an ultrabroadband millimeter-wavelength vector sliding correlator channel sounder and in-building measurements at 2.5 & 60 GHz'. MSc thesis, Virginia Polytechnic Institute and State University, 2002
2 Alejos, A.V.: 'Measurement, characterization and modeling of the radio channel for broadband multimedia systems at 40 GHz'. PhD thesis, Universidade de Vigo, 2006
3 Newhall, W.G.: 'Wideband propagation measurement results, simulation models, and processing techniques for a sliding correlator measurement system'. MSc thesis, Virginia Polytechnic Institute and State University, 1997
4 Takeuchi, T., Tamura, M.: 'A ultra-wide band channel sounder for mobile communication systems'. Twelveth IEEE Int. Symp. on Personal, Indoor and Mobile Radio Communications, San Diego, USA, 2001
5 Nie, S., MacCartney, G.R., Sun, S., Rappaport, T.S.: '28 GHz and 73 GHz signal outage study for millimeter wave cellular and backhaul communications'. IEEE Int. Conf. on Communications, Sydney, Australia, 2014
6 Cox, D.C.: 'Delay doppler characteristics of multipath propagation at 910 MHz in a suburban mobile radio environment', *IEEE Trans. Antennas Propag.*, 1972, **5**, pp. 625–635
7 Jeruchim, M.C., Balaban, P., Shanmugan, K.S.: 'Simulation of communication systems' (Plenum Press, 2000, 2nd edn.)
8 Newhall, W.G., Rappaport, T.S., Sweeney, D.G.: 'A spread spectrum sliding correlator system for propagation measurements'. RF Design, 1996, pp. 40–54
9 Parsons, J.D.: 'The mobile radio propagation channel' (John Wiley and Sons Inc., 1992)
10 Pirkl, R.J., Durgin, G.D.: 'Optimal sliding correlator channel sounder design', *IEEE Trans. Wirel. Commun.*, 2008, **9**, pp. 3488–3497
11 Ferreira, D., Caldeirinha, R.F.S.: 'Development and implementation of a real time high-resolution channel sounder – IF stage'. Vehicular Technology Conf., Budapest, Hungary, May 2011, pp. 1–5
12 Ferreira, D., Caldeirinha, R.F.S.: 'Development and performance analysis of a real time high-resolution channel sounder – IF stage'. EUROCON and Conftele, Lisbon, Portugal, April 2011, pp. 1–4
13 Ferreira, D., Caldeirinha, R.F.S.: 'Development and performance assessment of a real time high-resolution RF channel sounder'. Geoscience and Remote Sensing Symp., Vancouver, Canada, July 2011, pp. 1–4
14 Leonor, N., Ferreira, D., Caldeirinha, R., Fernandes, T.: 'Ray tracing based model using point scatterers for time-varying radio channels'. Conftele, Castelo Branco, Portugal, May 2013, pp. 1–4

© The Institution of Engineering and Technology 2015

17518733, 2015, 8, Downloaded from https://ietresearch.onlinelibrary.wiley.com/doi/10.1049/iet-map.2014.0165 by Instituto Politecnico De Leiria, Wiley Online Library on [18/10/2025]. See the Terms and Conditions (https://onlinelibrary.wiley.com/terms-and-conditions) on Wiley Online Library for rules of use; OA articles are governed by the applicable Creative Commons License